

## Poly(*N*-vinylpyrrolidone)이 그래프트된 Poly(3-hydroxybutyrate-*co*-3-hydroxyvalerate) 공중합체의 합성 및 결정화 거동

Wei Wang\*, Yu Zhang†, and Yanmo Chen

State Key Laboratory for Modification of Chemical Fiber & Polymeric Materials,  
College of Materials Science & Engineering, Donghua University, Shanghai 201620, PR China

\*College of Biological & Chemical Engineering, Jiaying University, Jiaying Zhejiang 314001, PR China  
(2007년 3월 22일 접수, 2007년 5월 9일 채택)

## Preparation and Crystallization Behavior of Poly(3-hydroxybutyrate-*co*-3-hydroxyvalerate) Grafted with Poly(*N*-vinylpyrrolidone)

Wei Wang\*, Yu Zhang†, and Yanmo Chen

State Key Laboratory for Modification of Chemical Fiber & Polymeric Materials,  
College of Materials Science & Engineering, Donghua University, Shanghai 201620, PR China

\*College of Biological & Chemical Engineering, Jiaying University, Jiaying Zhejiang 314001, PR China  
(Received March 22, 2007; Accepted May 9, 2007)

---

**Abstract :** Poly(*N*-vinylpyrrolidone) (PVP) groups were grafted onto a poly(3-hydroxybutyrate-*co*-3-hydroxyvalerate) (PHBV) backbone in order to modify its properties and synthesize a novel biocompatible copolymer. The crystallization behavior of PHBV and grafted PHBV was investigated by differential scanning calorimetry (DSC) and polarized optical microscopy (POM). During the cooling-induced crystallization process, the crystallization temperature and the crystallization rate of the grafted PHBV decreased with increasing PVP weight fraction. On the heating scans of all grafted PHBV samples, a new crystallization exothermic peak appeared at almost the same temperature, suggesting the operation of a recrystallization process, while the melting temperature ( $T_m$ ) and the apparent enthalpy of fusion ( $\Delta H_f$ ) were not affected by graft modification. During the isothermal crystallization process at the same temperature, the presence of side PVP groups decreased the spherulitic growth rate and the spherulitic band spacing with increasing PVP weight fraction in samples.

**Keywords :** poly(3-hydroxybutyrate-*co*-3-hydroxyvalerate) (PHBV), poly(*N*-vinylpyrrolidone) (PVP), graft modification, crystallization behavior, spherulitic growth rate.

---

### Introduction

Poly(3-hydroxybutyrate-*co*-3-hydroxyvalerate) (PHBV) is a thermoplastic polymer synthesized by microorganisms under imbalanced growth conditions, for example, in the presence of excess carbon source, and under nitrogen, magnesium or phosphor limited culture conditions. It serves as an intracellular storage product for carbon and energy, which can be utilized to support growth when an extracellular carbon source is absent. The synthesis of PHBV is very different from common polymers synthesized from petroleum or natural gas. PHBV can be synthesized by bacteria using different organic feedstocks, such as starch, waste edible

oils, waste vegetable, waste fruit and other organic wastes originating from industry and trade.<sup>1,2</sup> It can also be produced and extracted from plants, including Arabidopsis, through transgenic technology.<sup>3,4</sup> PHBV has many excellent properties, such as biodegradability, biocompatibility, piezoelectric property, and optical activity, which have supported its wide use as biodegradable packing materials, tissue engineering materials, drug delivery system and electric materials. With the shortage of energy resources and the increasing concern of environmental protection in world, the exploration and application of PHBV is attracting more and more research attention and industry interest.

The properties of PHBV can be tailored at a certain extent by varying the hydroxyvalerate (HV) content of the copolymer. At an HV content of 3–8 mol%, the thermal and

---

†To whom correspondence should be addressed.  
E-mail: zjxuwangwei@163.com

mechanical properties of PHBV are similar to those of polypropylene. PHBV can be processed in melting, and is therefore an environmentally friendly, prospective substitute for the currently used, non-biodegradable, thermoplastic resin. However, the present application of PHBV is very limited due to its inherent disadvantages such as high cost, hardness and brittleness, low thermal decomposition temperature, narrow processing window, and absence of functional groups. In order to improve the chemical, physical and processing properties of PHBV, various methods, including chemical modification<sup>5-8</sup> and blending with other polymers, have been investigated.<sup>9-12</sup> Among these modification methods, graft modification is a well-known method to both tailor the polymer properties and introduce the new functional groups to the same polymer backbone. Many studies on the graft modification of PHBV have also been reported.<sup>13-18</sup>

Poly(*N*-vinylpyrrolidone) (PVP) is a synthetically derived vinyl polymer with a unique combination of excellent properties, such as good solubility in water and a range of organic solvents, remarkable capacity to interact with a wide variety of organic and inorganic compounds, good biocompatibility, and non-toxicity to living tissues. PVP has been widely used in the biomedical, cosmetic and food industries which have been closely related to human health for decades. PVP has also been widely used as a medical additive or polymeric modifier.<sup>19-22</sup> If PVP could be grafted onto PHBV, not only would the properties of PHBV be improved but also new functional groups could be introduced. Meanwhile both substrate PHBV and grafted PVP groups are biocompatible, suggesting that the PHBV grafted with PVP will also have biocompatibility. These products could be used as biomaterials and could be further functionalized to extend their application because PVP groups have a remarkable capacity to interact with a wide variety of organic and inorganic compounds.

Although several polymers or monomers have been grafted onto PHBV, no grafting attempt has been reported with PVP. In this work, PVP groups were originally grafted onto PHBV using benzoyl peroxide (BPO) as an initiator in chlorobenzene to modify the properties of PHBV and synthesize a new novel, compatible copolymer which would combine the advantages of PHBV and PVP. The structure of raw PHBV and PHBV grafted with PVP was characterized by <sup>1</sup>H-NMR spectra. The crystallization behavior of raw PHBV and grafted PHBV was investigated by differential scanning calorimetry (DSC) and polarized optical microscopy (POM).

## Experimental

**Materials.** PHBV (Tian'an Bioproducts Ltd. Co., China; HV

content: 3.57 mol%, measured by <sup>1</sup>H-NMR) was recrystallized from ethanol and dried in a vacuum oven at 333 K for at least 24 h. *N*-vinylpyrrolidone (NVP, Fluka Chemika Ltd. Co., Germany) was treated with active carbon sorption to remove the inhibitor before use. BPO (Shanghai Zhongli Chemical Factory, China) was recrystallized from methanol. Chlorobenzene, hexamethylene (1,6-hexylidene), ethanol, methanol and PVP (PVP-K30), supplied by China Medicine Groups, were used as received.

**Preparation of PHBV Grafted with PVP.** Into 25 mL of chlorobenzene at above 373 K, 2.5 g of PHBV powder was completely dissolved in a three-neck flask. After the solution was cooled to room temperature, prescribed weights of NVP monomer and BPO initiator were added, and then the solution was heated up to a predetermined temperature under nitrogen atmosphere. Because all the feed stocks and products are soluble in chlorobenzene, this reaction is a kind of homogeneous solution copolymerization. After a chosen period of reaction, 100 mL of 1,6-hexylidene was poured into the solution while being stirred. The formed precipitates were filtered using a filter flask and dried at 333 K in a vacuum oven for at least 24 h. The rough products were extracted by ethanol in a Soxhlet apparatus for at least 48 h to ensure complete removal of the homopolymer PVP. Finally, the resultant precipitates were dried at 333 K in a vacuum oven for another 24 h and then weighed. The dried weight of the resultant products (*W*) should be higher than 2.5 g due to the grafting of the PVP groups onto PHBV. From the increased weight, the PVP weight fraction (PVP%) in the products was estimated according to the following equation:

$$\text{PVP\%} = \frac{W - 2.5}{2.5} \times 100 \quad (1)$$

Ethanol is a good solvent for PVP, as well as precipitant for raw PHBV and grafted PHBV, so the PVP homopolymer could be easily separated from the products. It should be noted here that unreacted PHBV was probably present in the products. However, in line with the modification intention, it was not necessary to separate the unreacted PHBV from the products. Therefore, blends of unreacted PHBV and the graft copolymer PHBV-*g*-PVP, with unknown composition, were actually obtained in this research. In several previous studies on polymer graft modification, the unreacted substrate polymer and graft copolymer were similarly not separated from the products.<sup>13-17, 23-25</sup>

In order to maximize the PVP% in the products, the orthogonal array design method, which will be reported in a separate paper, was adopted. The results showed that

**Table 1. Relationship between NVP in Feed and Result PVP% in Products**

NVP weight in feed(g)	Result PVP%
2.5	2.54
5.0	6.98
7.5	9.01
10.0	10.48

the optimal copolymerization conditions were as follows: reaction temperature of 393 K, reaction time of 1 h, BPO weight of 0.3 g, and NVP weight of 10 g. Under these optimized reaction conditions, the PVP% was maximized at 10.48%. Grafted PHBV samples with different PVP% were easily obtained by varying the weight of NVP in the feed (Table 1).

**<sup>1</sup>H-NMR Spectra Characterization.** The structural characterizations of the samples were determined by high-resolution <sup>1</sup>H-NMR spectra using a Bruker AU400 spectrometer. Deuterated chloroform was used as the solvent and tetramethylsilane (TMS) as the internal reference.

**DSC.** The crystallization and melting behaviors of all samples were analyzed by using DSC instrument. The instrument was calibrated with an indium standard ( $T_m=429.6$  K,  $\Delta H_f=28.5$  J/g) and the measurement was conducted under nitrogen atmosphere. The sample weight used in the DSC pan was maintained within 6–8 mg. The samples were first heated from room temperature to 463 K at a rate of 20 K/min, maintained there for 3 min to destroy all memories of the previous thermal and mechanic histories, cooled to room temperature at a rate of 10 K/min and finally heated to 463 K at the same rate. The temperature at the crystallization exothermic peak observed upon cooling from the melt ( $T_c$ ), the temperature at the crystallization exothermic peak observed upon heating from room temperature ( $T_{ch}$ ), and the melting temperature ( $T_m$ ) were determined from the DSC traces.

**POM.** The spherulitic growth rate ( $G$ ) and morphological structure of the samples were observed with an Olympus BX51 polarized optical microscope equipped with a hot stage. Each specimen was sandwiched between two thin glass slides, kept at 463 K for 3 min on the hot stage, and then cooling to the desired temperature as quickly as possible. The specimens were crystallized isothermally at a given temperature ( $T_c$ ). The growth rate of the spherulite radius was monitored as a function of time. The slope of the line obtained from the plot of the spherulitic radius versus time was taken to indicate the radial growth rate of the spherulites.

## Results and Discussion

**<sup>1</sup>H-NMR Spectra Characterization.** Figure 1 presents the <sup>1</sup>H-

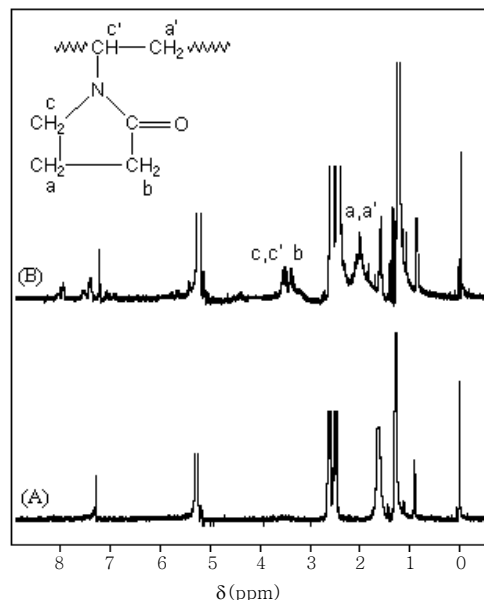


**Figure 1.** <sup>1</sup>H-NMR spectra of raw PHBV (A) and grafted PHBV with PVP% of 6.98% (B).

NMR spectra of raw PHBV (A) and grafted PHBV after ethanol extraction in a Soxhlet apparatus with the PVP% of 6.98% (B). Both spectra showed several characteristic peaks of methine protons at 5.25 ppm, methylene protons at 2.40–2.70 ppm, methyl protons of HB unit at 1.27 ppm and methyl protons of HV unit at 0.95 ppm, respectively. However, in the <sup>1</sup>H-NMR spectrum of the grafted PHBV sample, several distinct peaks appeared at about 2.00, 3.20, and 3.56 ppm, which were assigned to the protons of a(a'), b, and c(c') in the PVP unit, respectively, as shown in Figure 1 (B). In addition, the <sup>1</sup>H-NMR spectrum of the grafted PHBV exhibited the characteristic peak of aromatic ring protons at 7.45 ppm, which was probably due to the residue of the initiator. The HV content in PHBV (3.57 mol%) was determined from the ratio area of the peak at 0.95 ppm to that at 1.27 ppm.<sup>26</sup> The PVP weight fraction was estimated to be 7.02% from the ratio area of the peak at 2.00 ppm to that at 2.40–2.70 ppm, and was very near to the result calculated from eq. (1).

The <sup>1</sup>H-NMR structural characterizations indicated the presence of PVP groups in the grafted PHBV. In order to investigate the presence of a covalent bond between the PHBV backbone and PVP groups, 0.5 g of PVP-K30, 2.5 g of PHBV and 0.3 g of BPO were dissolved in 25 mL of chlorobenzene at 393 K under nitrogen atmosphere. After a 1-hr reaction time, 100 mL of hexamethylene was poured into the solution with stirring and the precipitates were formed. The precipitates were PHBV/PVP blends because hexamethylene is the *co*-precipitant for PHBV and PVP.

The blends were extracted by Soxhlet apparatus using ethanol for at least 48 h and then dried at 333 K in a vacuum oven for at least 24 h. The  $^1\text{H-NMR}$  spectrum of the PHBV/PVP blend sample after extraction was an almost identical copy of that of raw PHBV, confirming the complete extraction of PVP from the blends. Nevertheless, after the grafted PHBV was extracted once more at the same condition, the dried weight was maintained almost constant, as was the ratio area of the peak at 2.00 ppm to that at 2.40–2.70 ppm in the  $^1\text{H-NMR}$  spectra of sample before and after extraction. It is therefore reasonable to conclude that the presence of chemical bonding was more likely than covalent bonding between the PVP groups and PHBV substrate, i.e., that the PVP groups were successfully grafted onto the PHBV backbone.

**Crystallization Behavior of Raw PHBV and Grafted PHBV.** In order to study the effect of PVP weight fraction on the crystallization and melting behaviors of the grafted PHBV, samples with PVP% given in parentheses were selected as follows: PHBV-*g*-PVP(2.54), PHBV-*g*-PVP(6.98), PHBV-*g*-PVP(9.01), and PHBV-*g*-PVP(10.48).

Figure 2 shows the crystallization behavior of raw PHBV

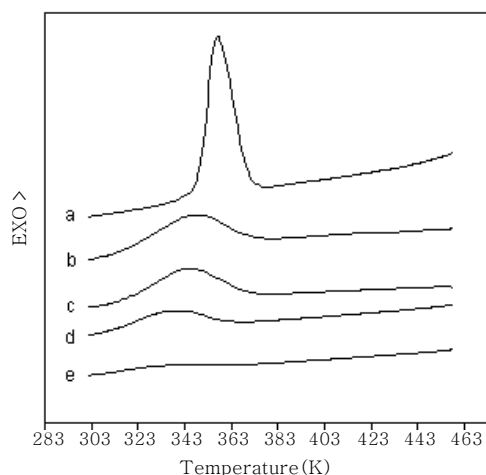


**Figure 2.** DSC traces of raw PHBV and grafted PHBV with different PVP% crystallized from the melt at a cooling rate of 10 K/min. (a) raw PHBV, (b) PHBV-*g*-PVP(2.54), (c) PHBV-*g*-PVP(6.98), (d) PHBV-*g*-PVP(9.01), and (e) PHBV-*g*-PVP(10.48).

and grafted PHBV with different PVP%, while Table 2 shows the parameters of the crystallization process. At the temperature of crystallization exotherm peak upon cooling ( $T_{cc}$ ), the value of the heat flow was maximized. The initial slope of the exotherm peak ( $S_1$ ), which is the slope at inflexion on the high temperature side of the peak, is positively correlated to the nucleation rate.  $T_{cc(\text{onset})}$  is the temperature at the intersection of the tangent at the baseline and the high temperature side of the peak. The width at half height of the exotherm peak ( $\Delta W$ ) is determined after normalized of the peak to a constant sample mass. A smaller  $\Delta W$  value indicates a narrower crystallite size distribution. The parameter  $T_{cc(\text{onset})} - T_{cc}$  is a measure of the overall rate of crystallization, with a smaller  $T_{cc(\text{onset})} - T_{cc}$  value indicating a higher crystallization rate.<sup>27</sup>

The results showed that  $T_{cc}$  of the grafted PHBV samples was remarkably decreased as a function of PVP% in comparison with raw PHBV.  $T_{cc(\text{onset})}$  of grafted PHBV decreased slightly with increasing PVP%. These results indicated that the PVP side groups hindered the crystallization process of the grafted samples. It is clear that the sample values of  $T_{cc(\text{onset})} - T_{cc}$  increased with increasing PVP%, which offers further proof that the crystallization process is hindered by the introduction of PVP groups into the PHBV backbone. The PVP groups reduced the crystallization rate and increased the steric hindrance for the regular folding of grafted PHBV molecular chains.

Table 2 also confirmed that  $S_1$  decreased with increasing PVP%, implying that samples with lower PVP% had a greater nucleation rate. Hence, the crystallites size distribution of the samples with lower PVP% should be smaller than that of those with higher PVP%. This analysis agrees with the increase in the calculated value of  $\Delta W$  with increasing PVP%. The PVP groups may have reduced the nucleation and crystallization rate of the grafted samples, thereby increasing the crystallite size distribution.

**Melting Behavior of Raw PHBV and Grafted PHBV.** Figure 3, showing the DSC traces of raw PHBV and grafted PHBV with different PVP% on heating, exhibits two melting endothermic peaks on the DSC curve of raw PHBV due to its unusual

**Table 2. Crystallization Parameters of Raw PHBV and Grafted PHBV with Different PVP%**

Samples	$T_{cc}$ (K)	$T_{cc(\text{onset})}$ (K)	$T_{cc(\text{onset})} - T_{cc}$ (K)	$\Delta W$ (K)	$-\Delta H_{cc}$ (J/g) <sup>a</sup>	$S_1$
Raw PHBV	357.5	373.3	15.8	12.8	61.33	7.64
PHBV- <i>g</i> -PVP(2.54)	348.2	372.7	24.5	29.7	30.62	1.87
PHBV- <i>g</i> -PVP(6.98)	344.7	371.5	26.8	30.3	28.21	1.09
PHBV- <i>g</i> -PVP(9.01)	341.2	368.5	27.3	33.8	18.58	0.72
PHBV- <i>g</i> -PVP(10.48) <sup>b</sup>	334.2	368.0	33.8	38.5	5.67	0.22

<sup>a</sup> $\Delta H_{cc}$  = enthalpy of crystallization upon cooling. <sup>b</sup>Peak obtained from the enlarged DSC trace.

*co*-crystallization phenomena,<sup>28,29</sup> but only one peak on the DSC curves of all grafted PHBV samples, indicating the disappearance of the *co*-crystallization phenomena. It is noteworthy that a new exothermic peak appeared at almost the same temperature (323–324 K) in the DSC curves of all grafted PHBV samples, regardless of the PVP%. This new peak temperature, termed  $T_{ch}$  as it indicates the temperature at the crystallization exotherm peak upon heating, has not previously been reported in the research on PHBV and modified PHBV. The appearance of  $T_{ch}$  was ascribed to the recrystallization process of grafted PHBV upon heating because of its weakened crystallization ability upon cooling. The crystallization rate of raw PHBV upon cooling is relatively high, indicating that the crystallization process is mainly completed before the sample is cooled down to room temperature. However, as noted above the crystallization rate of grafted PHBV is relatively low and the crystallization process can not be completed, which allows many imperfect spherulites and crystal nuclei to form upon cooling. These imperfect crystals and nuclei could not grow at low temperature. When the samples were heated to a suitable tem-

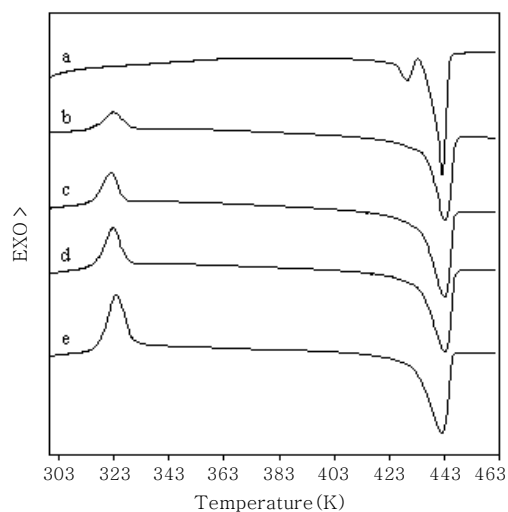


**Figure 3.** DSC traces of raw PHBV and grafted PHBV with different PVP% at a heating rate of 10 K/min. (a) raw PHBV, (b) PHBV-*g*-PVP(2.54), (c) PHBV-*g*-PVP(6.98), (d) PHBV-*g*-PVP(9.01), and (e) PHBV-*g*-PVP(10.48).

perature, these imperfect crystals and nuclei grew again, allowing recrystallization to occur and a new crystallization exothermic peak to appear.

The melting parameters of the samples are shown in Table 3. At the temperature of the recrystallization exotherm peak upon heating ( $T_{ch}$ ), the value of the heat flow was maximized similar to the crystallization process upon cooling. The initial slope of the exotherm peak ( $S_2$ ), i.e., the slope at inflexion on the low temperature side of the exotherm peak, which can be considered to be a measurement of the nucleation rate on heating, is also a function of PVP%, but with a trend contrary to that of  $S_1$ : with increasing PVP%,  $S_2$  increased, while  $S_1$  decreased (Figure 4). The same phenomenon was also observed for  $-\Delta H_{ch}$ , the enthalpy of recrystallization upon heating, and for  $-\Delta H_{cc}$ , the enthalpy of crystallization upon cooling (Figure 5). These results indicated that with decreasing crystallization rate, more imperfect spherulites and crystal nuclei formed on cooling, and therefore that the recrystallization rate increased and the recrystallization enthalpy increased with heating.

Although the crystallization capability of the grafted PHBV decreased with increasing PVP%, the apparent enthalpy of fusion ( $\Delta H_f$ ) of all samples remained almost constant, implying an unchanged degree of crystallization, probably due to the recrystallization process before melting for the grafted PHBV on heating. The undercooling temperature,  $\Delta T = T_m - T_{cc}$ , was used to describe the kinetic crystallization ability during non-isothermal crystallization process. A higher  $\Delta T$  suggested a

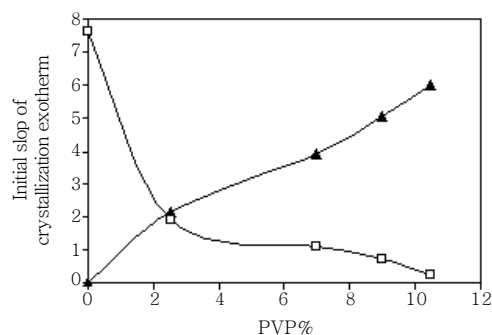


**Figure 4.**  $S_1$  (□) and  $S_2$  (▲) vs PVP%.

**Table 3.** Melting Parameters of Raw PHBV and Grafted PHBV with Different PVP%

Samples	$T_{ch}$ (K)	$-\Delta H_{ch}$ (J/g) <sup>a</sup>	$S_2$	$T_m$ (K)	$-\Delta H_f$ (J/g) <sup>b</sup>	$T_m - T_{cc}$ (K)	$T_{cc} - T_{ch}$ (K)
Raw PHBV	— <sup>c</sup>	0	0	442.7	68.92	85.2	— <sup>c</sup>
PHBV- <i>g</i> -PVP(2.54)	323.1	15.09	2.14	443.8	70.71	95.6	25.1
PHBV- <i>g</i> -PVP(6.98)	323.7	24.32	3.91	444.4	69.40	99.7	21.0
PHBV- <i>g</i> -PVP(9.01)	323.1	41.65	5.08	443.8	69.40	102.6	18.1
PHBV- <i>g</i> -PVP(10.48)	323.3	50.04	6.01	443.3	68.47	109.1	10.9

<sup>a</sup> $\Delta H_{ch}$  = Enthalpy of crystallization upon cooling. <sup>b</sup> $\Delta H_f$  = Apparent enthalpy of fusion. <sup>c</sup>Not be detected.

lower kinetic crystallization ability in the range from  $T_m$  to  $T_g$ . As shown in Table 3,  $T_m$  of all samples was almost unchanged, whereas the value of  $T_m - T_{cc}$  increased with increasing PVP%, implying that the rate of chain addition to the growing crystal may have been hindered by PVP side groups. The same conclusion is reached by examining the quantity of  $T_{cc} - T_{ch}$ , which can be considered to indicate the relative rate of crystallization of the sample,<sup>30</sup> as this value showed a monotonic decrease with increasing PVP%. Further crystal growth rate studies should focus on a more complete interpretation of these data.

Isothermally Crystallized Spherulities of PHBV and Grafted PHBV. In this work, the spherulitic growth rates ( $G$ ) of the samples isothermally crystallized at different crystallization

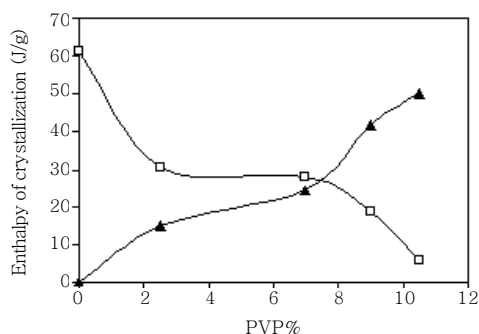


**Figure 5.**  $-\Delta H_{cc}$  ( $\square$ ) and  $-\Delta H_{ch}$  ( $\blacktriangle$ ) vs PVP%.

temperatures ( $T_c$ ) were determined with POM.  $T_c$  ranged from 333 to 373 K. Figure 6 shows the dependence of  $G$  on  $T_c$  for all samples. The figure clearly shows the  $G$  peak value for all samples at a certain temperature ( $T_{max}$ ).  $T_{max}$  was about 363 K for raw PHBV, but decreased by about 10–15 K for grafted PHBV. The spherulitic growth rates of the grafted PHBV samples decreased with increasing PVP% at the same  $T_c$ , indicating that the presence of PVP side groups reduced the spherulitic growth rate of the grafted PHBV samples, presumably caused by the decreased segmental

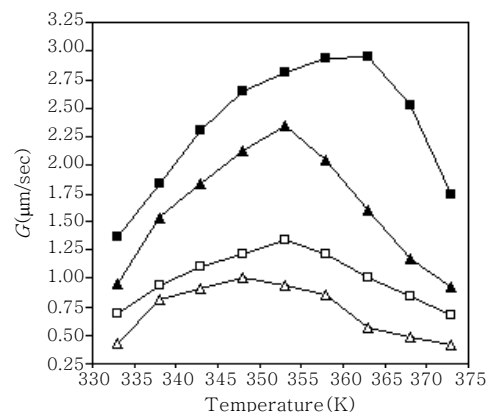


**Figure 6.** Spherulitic growth rate ( $G$ ) as a function of  $T_c$  for raw PHBV and Grafted PHBV.  $\blacksquare$ —Raw PHBV,  $\blacktriangle$ —PHBV-*g*-PVP(2.54),  $\square$ —PHBV-*g*-PVP(6.98),  $\triangle$ —PHBV-*g*-PVP(9.01).

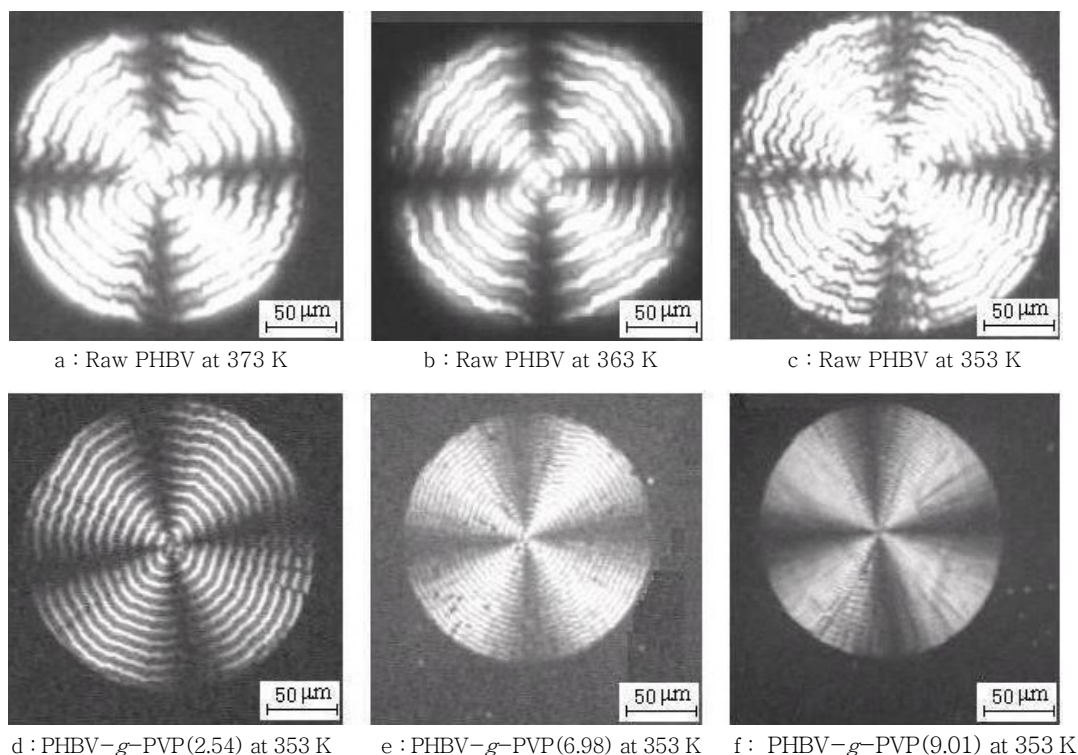


**Figure 7.** A series of polarized optical micrographs for samples isothermally crystallized at different temperatures.

mobility for the grafted PHBV due to the steric hindrance effect of the PVP side groups.

Figure 7 shows a series of polarized optical micrographs of samples isothermally crystallized at different crystallization temperatures. The figure indicates that all spherulites exhibited a typical black cross with a banded structure and an absence of cracks. The band spacing changed with isothermal crystallization temperature and PVP%. For raw PHBV, the band spacing decreased with decreasing crystallization temperature (Figures 7(a)–(c)). At the same crystallization temperature, the band spacing decreased with increasing PVP% (Figures 7(c)–(f)). Generally, the banded structure of spherulite is caused by the presence of twisted lamellae which result from the stress generated during crystallization and probably occurring within the disordered fold surfaces of the polymer crystals.<sup>31,32</sup> Hence one possible explanation for this change of band spacing in the spherulites is the effect of the PVP side groups in inducing stress on the lamellar surfaces of the grafted PHBV samples.

## Conclusions

PVP groups were successfully grafted onto PHBV substrate using BPO as an initiator in chlorobenzene under nitrogen atmosphere. The PVP% peaked at 10.48% under the optimal reaction conditions and grafted PHBV samples with different PVP% could be tailored by varying the NVP weight in the feed. The structures of the raw PHBV and the grafted PHBV with PVP% of 6.98% were characterized by <sup>1</sup>H-NMR spectra. Chemical bonding between the PVP groups and the PHBV substrate was considered more likely than covalent bonding based on the comparative analysis of weight reduction and <sup>1</sup>H-NMR spectra change of the grafted samples and the blend samples after selective extraction.

The crystallization and melting behaviors of raw PHBV and grafted PHBV with different PVP% were investigated by DSC. In comparison with raw PHBV, the crystallization and melting behaviors of grafted PHBV differed markedly depending on PVP%. The crystallization temperature on cooling ( $T_c$ ), and the crystallization and nucleation rate of grafted PHBV samples upon cooling all decreased with increasing PVP%, suggesting a weakened crystallization capability of the grafted samples upon cooling due to steric hindrance.  $T_m$  of all samples was almost constant, but the two characteristic melting endothermic peaks of raw PHBV disappeared in the heating DSC traces of all grafted PHBV samples, indicating the absence of any *co*-crystallization phenomena in the grafted samples. A new crystallization exothermic peak ( $T_{ch}$ ) appeared on the heating scans of all

grafted PHBV samples, but its position was almost unchanged, indicating that the recrystallization process occurred at a suitable temperature before melting of the grafted PHBV samples. In contrast to the crystallization process on cooling, the initial slope at inflexion on the low temperature side of the recrystallization exothermic peak ( $S_2$ ) and the enthalpy of recrystallization ( $-ΔH_{ch}$ ) upon heating both increased with increasing PVP%, indicating an increased recrystallization and nucleation rate upon heating for the grafted PHBV at higher PVP%. Although the crystallization capability of the grafted PHBV samples decreased with increasing PVP%, the apparent enthalpy of fusion ( $ΔH_f$ ), which is related to the crystallization degree, remained almost constant for all samples due to the recrystallization process for the grafted PHBV samples before melting.

In the POM investigation of the isothermal crystallization process of the raw PHBV and grafted PHBV samples, all spherulites exhibited a typical black cross with a banded structure and an absence of cracks. For raw PHBV, the band spacing decreased with decreasing crystallization temperature. At the same crystallization temperature, the band spacing decreased with increasing PVP%. The spherulitic growth rates ( $G$ ) of the grafted samples decreased with increasing PVP% at the given crystallization temperature and  $T_{max}$  decreased by about 10–15 K for the grafted PHBV samples.

**Acknowledgments :** This research was supported by the Shanghai Dawn Project (No.2000SG27) and the Key Project of the Educational Ministry of China (No.00059).

## References

1. K. J. Ganzeveld, A. V. Haen, M. H. V. Agteren, W. D. Koning, and A. J. M. Schoot Uiterkamp, *J. Clean Prod.*, **7**, 413 (1999).
2. I. Taniguchi, K. Kagotani, and Y. Kimura, *Green Chem.*, **5**, 545 (2003).
3. H. X. Sun, Y. H. Wang, Z. Y. Wu, Q. K. Yang, W. B. Li, and C. L. Huang, *Biotechnol. Bull.*, **2**, 5 (2004).
4. T. Wang, L. Ye, and Y. R. Song, *Chinese Sci. Bull.*, **44**, 1729 (1999).
5. P. D. Haene, E. E. Remsen, and J. Asrar, *Macromolecules*, **32**, 5229 (1999).
6. B. Fei, C. Chen, S. Chen, S. W. Peng, Y. G. Zhuang, Y. X. An, and L. S. Dong, *Polym. Int.*, **53**, 937 (2004).
7. A. Mas, H. Jaaba, and F. Schue, *J. Macromol. Sci.; Pure Appl. Chem.*, **A34**, 67 (1997).
8. I. Gursel, C. Balcik, Y. Arica, O. Akkus, N. Akkas, and V. Hasirci, *Biomaterials*, **19**, 1137 (1998).
9. Y. S. Chun and W. N. Kim, *Polymer*, **41**, 2305 (2000).

10. Z. B. Qiu, T. Ikehara, and T. Nishi, *Polymer*, **44**, 7519 (2003).
11. Z. B. Qiu, S. Fujinamib, M. Komurab, K. Nakajimab, T. Ikehara, and T. Nishi, *Polymer*, **45**, 4355 (2004).
12. Y. He, N. Asakawa, and Y. Inoue, *J. Polym. Sci.; Part B: Polym. Phys.*, **38**, 2891 (2000).
13. H. S. Lee and T. Y. Lee, *Polymer*, **38**, 4505 (1997).
14. Y. Tesema, D. Raghavan, and III J. Stubbs, *J. Appl. Polym. Sci.*, **93**, 2445 (2004).
15. S. G. Hu, C. H. Jou, and M. C. Yang, *Biomaterials*, **24**, 2685 (2003).
16. S. G. Hu, C. H. Jou, and M. C. Yang, *J. Appl. Polym. Sci.*, **88**, 2797 (2003).
17. K. Fujimoto, Y. Takebayashi, H. Inoue, and Y. Ikada, *J. Polym. Sci.; Part A: Polym. Chem.*, **31**, 1035 (1993).
18. J. Park, J. G. Park, W. M. Choi, C. S. Ha, and W. J. Cho, *J. Appl. Polym. Sci.*, **74**, 1432 (1999).
19. M. Källrot, U. Edlund, and A. C. Albertsson, *Biomaterials*, **27**, 1788 (2006).
20. Y. Zhang and Y. M. Lam, *J. Colloid. Interf. Sci.*, 285, 80 (2005).
21. S. E. Cook, I. K. Park, E. M. Kim, H. Jeong, T. G. Park, Y. Jaie, T. Akaikea, and C. S. Cho, *J. Control. Release*, **105**, 151 (2005).
22. I. K. Park, J. E. Ihm, Y. H. Park, Y. J. Choi, S. I. Kim, W. J. Kim, T. Akaike, and C. S. Cho, *J. Control. Release*, **86**, 349 (2003).
23. L. L. Wang and Y. S. Xu, *Iran. Polym. J.*, **15**, 467 (2006).
24. J. L. Willett, M. A. Kotnis, G. S. O'Brien, G. F. Fanta, and S. H. Gordon, *J. Appl. Polym. Sci.*, **70**, 1121 (1998).
25. P. Manaresi, V. Passalacqua, and F. Pilati, *Polymer*, **16**, 520 (1975).
26. S. Bloembergen, D. A. Holden, G. K. Hamer, T. L. Bluhm, and R. H. Marchessault, *Macromolecules*, **19**, 2865 (1986).
27. J. Li, M. F. Lai, and J. J. Liu, *J. Appl. Polym. Sci.*, **92**, 2514 (2004).
28. M. Scandola, G. Ceccorulli, M. Pizzoli, and M. Gazzano, *Macromolecules*, **25**, 1405 (1992).
29. T. L. Bluhm, G. K. Hamer, R. H. Marchessault, C. A. Fyfe, and R. P. Veregin, *Macromolecules*, **19**, 2871 (1986).
30. D. R. Fagerburg, J. J. Watkins, and P. B. Lawrence, *Macromolecules*, **26**, 114 (1993).
31. P. X. Xing, L. S. Dong, Y. X. An, and Z. L. Feng, *Macromolecules*, **30**, 2726 (1997).
32. B. Fei, C. Chen, H. Wu, S. W. Peng, X. Y. Wang, L. S. Dong, and J. H. Xin, *Polymer*, **45**, 6275 (2004).